

6. Parker, G. A. & Begon, M. Optimal egg size and clutch size: effects of environment and maternal phenotype. *Am. Nat.* **128**, 573–592 (1986).
7. Lloyd, D. C. Selection of offspring size at independence and other size-versus-number strategies. *Am. Nat.* **129**, 800–817 (1987).
8. McGinley, M. A., Temme, D. H. & Geber, M. A. Parental investment in offspring in variable environments: theoretical and empirical considerations. *Am. Nat.* **130**, 370–398 (1987).
9. Sargent, R. C., Taylor, P. D. & Gross, M. R. Parental care and the evolution of egg size in fishes. *Am. Nat.* **129**, 32–46 (1987).
10. Geritz, S. A. H. Evolutionary stable seed polymorphism and small-scale spatial variation in seedling density. *Am. Nat.* **146**, 685–707 (1995).
11. Bernardo, J. The particular maternal effect of propagule size, especially egg size: patterns, models, quality of evidence and interpretations. *Am. Zool.* **36**, 216–236 (1996).
12. Sinervo, B., Doughty, P., Huey, R. B. & Zamudio, K. Allometric engineering: a causal analysis of natural selection on offspring size. *Science* **258**, 1927–1930 (1992).
13. Elgar, M. A. Evolutionary compromise between a few large and many small eggs: comparative evidence in teleost fish. *Oikos* **59**, 283–287 (1990).
14. Sinervo, B. & Licht, P. Proximate constraints on the evolution of egg size, number, and total clutch mass in lizards. *Science* **252**, 1300–1302 (1991).
15. Fleming, I. A. Reproductive strategies of Atlantic salmon: ecology and evolution. *Rev. Fish Biol. Fish.* **6**, 379–416 (1996).
16. Wade, M. J. & Kalisz, S. The causes of natural selection. *Evolution* **44**, 1947–1955 (1990).
17. Sinervo, B. & Svensson, E. Mechanistic and selective causes of life history trade-offs and plasticity. *Oikos* **83**, 432–442 (1998).
18. Jonsson, N., Jonsson, B. & Fleming, I. A. Does early growth cause a phenotypically plastic response in egg production of Atlantic salmon? *Funct. Ecol.* **10**, 89–96 (1996).
19. Kamler, E. *Early Life History of Fish: an Energetics Approach* (Chapman & Hall, London, 1992).
20. Einum, S. & Fleming, I. A. Genetic divergence and interactions in the wild among native, farmed and hybrid Atlantic salmon. *J. Fish Biol.* **50**, 634–651 (1997).
21. Lande, R. & Arnold, S. J. The measurement of selection on correlated characters. *Evolution* **37**, 1210–1226 (1983).

**Acknowledgements**

We thank J. G. Backer, K. Bergersen, T. Husebø and the rest of the staff at the NINA Research Station, Ims, for assistance with the experiments. We also thank J. D. Armstrong, P. Fiske, T. Forseth, A. P. Hendry, K. Hindar, B. Jonsson and O. Ugedal for comments on the manuscript. Financial support was provided by a PhD scholarship from the Norwegian Research Council to S.E. and research funding from the Norwegian Institute for Nature Research to I.A.F.

Correspondence and requests for materials should be addressed to S.E. (e-mail: sigurd.einum@ninatrd.ninaniku.no).

**Cortical ensemble activity increasingly predicts behaviour outcomes during learning of a motor task**

**Mark Laubach, Johan Wessberg & Miguel A. L. Nicolelis**

*Department of Neurobiology, Duke University Medical Centre, Durham, North Carolina 27710, USA*

When an animal learns to make movements in response to different stimuli, changes in activity in the motor cortex seem to accompany and underlie this learning<sup>1–6</sup>. The precise nature of modifications in cortical motor areas during the initial stages of motor learning, however, is largely unknown. Here we address this issue by chronically recording from neuronal ensembles located in the rat motor cortex, throughout the period required for rats to learn a reaction-time task. Motor learning was demonstrated by a decrease in the variance of the rats' reaction times and an increase in the time the animals were able to wait for a trigger stimulus. These behavioural changes were correlated with a significant increase in our ability to predict the correct or incorrect outcome of single trials based on three measures of neuronal ensemble activity: average firing rate, temporal patterns of firing, and correlated firing. This increase in prediction indicates that an association between sensory cues and movement

emerged in the motor cortex as the task was learned. Such modifications in cortical ensemble activity may be critical for the initial learning of motor tasks.

Traditional theories of cortical function propose that information in the central nervous system is represented primarily by the firing rate of single neurons<sup>7,8</sup>. Learning new motor contingencies should therefore primarily involve changes in the average firing of neurons located in sensorimotor cortical areas. Behaviourally relevant information can also be represented in temporal patterns of neuronal firing (on a ms scale) and correlated neuronal activity<sup>9–15</sup>. It is not known whether these other schemes of neuronal representation are significant in the physiological modifications associated with the initial learning of a motor task. To address this issue, we compared the potential contribution of three neuronal coding schemes (average firing rate, temporal patterns of firing, and correlated activity) for predicting the behavioural outcome of single trials throughout the period required for rats to learn a reaction-time task. We also compared concurrent neural ensemble and electromyography (EMG) recordings to establish that any increase in single trial prediction by ensemble activity was not due to differences in movements on the correct and error trials.

Rats were trained to perform a reaction-time task in which they were required to hold down a response lever throughout a variable interval (the foreperiod, 400–800 ms) and to release the lever in response to vibrotactile or auditory trigger stimuli with a short (< 1 s) reaction time (Fig. 1a). Correct trials occurred when the rats sustained the lever press until the presentation of the trigger stimuli and released the lever with a short reaction time. Error trials occurred when the rats released the lever before the trigger stimulus. During the first of week of training, the rats exhibited significant increases in the time they were able to wait for the trigger stimulus, from 422.3 ± 30.9 ms (day 1) to 577.8 ± 24.8 ms (day 7; repeated-measures analysis of variants (ANOVA): *P* < 10<sup>-4</sup>; Fig. 1b). Although the rats' reaction times during these sessions did not change (day 1: 320.8 ± 41.5 ms; day 7: 271.6 ± 32.9 ms;

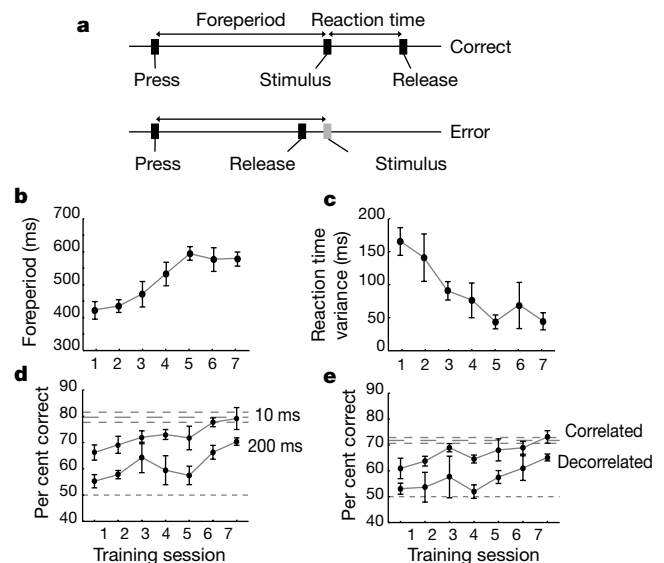


**Figure 1** Improvements in behavioural performance paralleled increases in the neuronal predictions of trial outcomes. **a–c**, As the rats learned the task (**a**), they sustained lever presses over longer foreperiods (**b**) and exhibited decreased variance in their reaction times (**c**). **d**, Predictions of trial outcomes based on neuronal activity increased with training and, by day 6–7, achieved levels equal to those in fully trained rats (upper lines, mean ± s.e.m.). Chance discrimination was 50% (lower dashed line). Temporal patterns of firing (from smoothing over 10-ms intervals) predicted trial outcomes better than average firing rates (combined over 200 ms). Likewise, predictions based on correlated firing were significantly better than those based on decorrelated ensemble activity.

repeated-measures ANOVA:  $P > 0.05$ ), the variance of the rats' reaction times decreased significantly (day 1:  $165 \pm 24.2$  ms; day 7:  $44.5 \pm 6.6$  ms; repeated-measures ANOVA:  $P < 0.02$ ; Fig. 1c). After these training sessions, our animals performed the task as well as animals in previous studies of reaction-time behaviour in rats, that is, better than 70% correct trials<sup>16</sup>.

Chronic and simultaneous recordings were obtained from neurons ( $25.4 \pm 1.3$  neurons per session, mean  $\pm$  s.e.m., range 14 to 32 neurons, total 711) in the forelimb representation of two motor areas of the cerebral cortex (medial and lateral agranular cortical areas, mAG and lAG) of six rats. To study the effect of learning on neuronal activity, spike trains in the 200-ms interval before lever release were compared for correct and error trials. The capability of three different types of neuronal coding schemes to predict the outcomes of single trials as correct or error was quantified using artificial neural network (ANN) methods<sup>17,18</sup>. The ANNs were trained with neuronal ensemble responses from subsets of trials and tested with the remaining trials (Fig. 2) for each training session throughout the learning period. The degree to which confusion matrices from the ANNs differed from chance was then evaluated using information theory<sup>19</sup> and was expressed as bits of information.

The majority of cortical neurons (477, 67.1%) were active when the rats pressed and released the lever (Fig. 2). However, over the seven training sessions, the responses of only nine of these neurons provided more than 0.1 bits of information about trial outcome. That is, 98.1% of the single neurons alone did not predict trial outcome accurately (overall average of  $59.3 \pm 0.3\%$  correct,  $0.015 \pm 0.001$  bits for all training sessions). The average amount of information represented by the single neurons was  $0.011 \pm 0.001$  bits on the first day of training and  $0.024 \pm 0.004$  bits on the seventh day of training. Permutation tests<sup>20</sup> showed that these information values are not statistically significant and can be generated by chance alone.

By contrast, predictions of trial outcome based on the average firing rate (using a single 200-ms bin) of the same cortical neurons analysed together as ensembles improved significantly in the first seven days of training, from  $55.3 \pm 2.5\%$  ( $0.013 \pm 0.004$  bits, day 1) to  $70.3 \pm 1.4\%$  ( $0.073 \pm 0.017$  bits, day 7,  $P < 0.01$ , repeated measures ANOVA, Fig. 1d). While the amount of information represented by average ensemble firing rate on the seventh day of training was small, permutation tests showed that it was highly significant ( $P \approx 0.30$ , day 1;  $P = 0.02$ , day 7). This improvement in trial prediction over learning occurred in the absence of any significant change in overall firing rates for the neuronal ensembles ( $20.6 \pm 1.6$  Hz for all sessions, Kruskal–Wallis test:  $P = 0.573$ ).

Next, we observed that single trial classification improved significantly when neuronal spike trains were smoothed over 10-ms intervals (Fig. 3a), from  $66.2 \pm 2.9\%$  ( $0.087 \pm 0.020$  bits, day 1) to  $79.1 \pm 4.2\%$  of the trials correct ( $0.227 \pm 0.060$  bits, day 7). This corresponded to more than a 200% increase in trial prediction based on information theory ( $P < 0.01$ , repeated measures ANOVA, Fig. 1d). Predictions based on fine temporal patterns of firing (10-ms intervals) on the seventh day of training yielded three times more information than average firing rates (200-ms interval) and were better than those based on average firing rates for all days of training (ANOVA:  $P < 10^{-4}$ ). In fully trained animals ( $n = 6$ ), the outcomes of single trials were predicted equally well if spikes were smoothed over 5-ms intervals ( $79.6 \pm 1.9\%$  correct,  $0.207 \pm 0.032$  bits) or 10 ms ( $77.3 \pm 1.4\%$ ,  $0.178 \pm 0.025$  bits). However, predictions were significantly worse (ANOVA:  $P < 0.005$ ) when spikes were smoothed over 20-ms intervals ( $71.8 \pm 0.7\%$  correct,  $0.105 \pm 0.008$  bits) or combined over 200 ms ( $63.6 \pm 1.9\%$  correct,  $0.038 \pm 0.011$  bits). These results indicate that fine temporal integration (10 ms or less) of firing across an ensemble of cortical neurons may encode the contingency between trigger stimuli and movement execution.

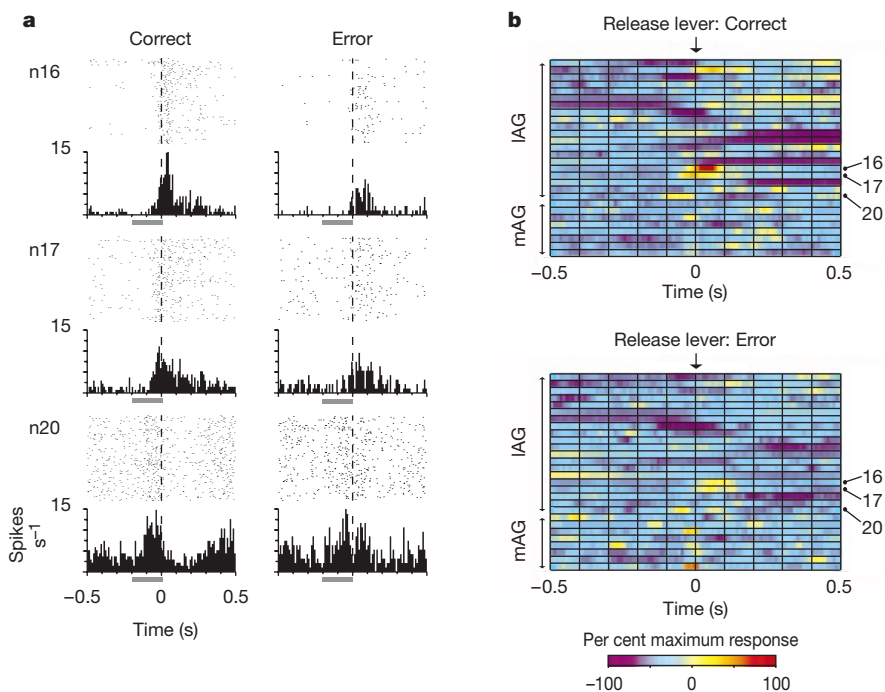


**Figure 2** Neuronal ensemble responses associated with correct and error trials. **a**, Single neurons ( $n$ ) in the lateral (lAG) and medial (mAG) agranular areas of motor cortex fired differently on correct and error trials (bin, 10 ms). The bars below each plot show the 200-ms period analysed in this study. **b**, Different temporal modulations of firing on correct and

error trials occurred over the neuronal ensembles around lever release (time = 0). Each horizontal line represents the firing of a neuron over time (in seconds). Neuronal firing was normalized to be  $-100$  (purple) to  $+100\%$  (red) of the maximum firing rate in the ensemble (bin, 10 ms; responses smoothed with a 5-ms moving average filter).

We also measured how well correlated firing predicted single trial outcomes over the course of learning. Independent component analysis (ICA; refs 21, 22) was used to quantify zero-lag correlations between groups of neurons (Fig. 3b). Prediction of single trial outcome based on the independent components improved significantly over learning, from  $60.9 \pm 4.0\%$  ( $0.049 \pm 0.022$  bits on day 1) to  $73.1 \pm 2.4\%$  ( $0.167 \pm 0.044$  bits on day 7, repeated measures ANOVA:  $P < 0.01$ , Fig. 1e), and provided more than twice the information obtained from average firing rate. The amount of covariance accounted for by the independent components did not change over the training period (day 1:  $42.6 \pm 2.3\%$ ; day 7:  $45.0 \pm 4.5\%$ ; repeated measures ANOVA:  $P = 0.85$ ). This result indicates that although the degree of correlated activity within the ensembles did not change, the information about trial outcome contained in the correlated activity increased with learning. The distributions of the independent components over the neuronal ensembles revealed patterns of correlated firing by subsets of the neurons that were not equally distributed across the motor cortex (Fig. 3b).

To demonstrate further that the information accounted for by ICA was due to correlated firing, a ‘spike-shifting’ procedure was used to reduce correlations across the neuronal ensemble without altering the firing rates of the individual neurons. This procedure resulted in a significantly lower percentage of correctly classified trials by the ANNs throughout learning ( $n = 4$ ,  $P < 0.001$ , Fig. 1e). These values of information were not significantly different from those obtained with the average firing rates of the same ensembles (Student’s  $t$ -test:  $P > 0.05$ ). Thus, correlated firing, as detected by ICA, proved to be a potential means of encoding information in addition to that available in average neuronal ensemble firing rates.

One possible confound for this study was that the occurrence of sensory stimuli on correct but not error trials could have been the

basis of the discriminations. However, several results discount this possibility. First, very few neurons exhibited any response to the vibrotactile and none to the auditory stimuli. Second, in the rare occasions when a tactile response was observed, the latency and duration of the responses were brief. As our data analysis interval was 200 ms before movement onset, and the average reaction time was  $271.6 \pm 32.9$  ms (day 7), these short-lasting tactile responses did not have a major impact on our analyses. Also, the time interval accounting for most of the single trial prediction (Figs 2 and 3) occurred 100 ms before movement onset. Thus, it seems unlikely that sensory responses of the cortical neurons accounted for the improvement in trial prediction observed over learning.

Another potential confound is that the cortical neuronal patterns that produce predictions of single trials may have reflected differences in motor output between correct and error trials. Several types of control data imply that this is not probable. First, video recordings of the animals showed no difference in overt behaviour between the types of trials. Second, there was no statistical difference in lever trajectories between correct and error trials. Third, EMG activity (Fig. 4a, b), recorded from several of the main muscles involved in lever release in two control animals, provided insignificant amounts of information about whether a single trial was correct or not (rat 1, 2 muscles:  $62.2 \pm 2.0\%$  correct,  $0.008 \pm 0.003$  bits; rat 2, four muscles:  $61.8 \pm 1.1\%$  correct,  $0.029 \pm 0.007$  bits;  $P > 0.1$ ; Fig. 4c). Fourth, in both control animals, single trial classification achieved using groups of muscles was not better than that obtained using the best individual muscle in each animal (that is, there was no additive effect across muscles). Finally, when neuronal ensemble activity in motor cortex was recorded simultaneously with multiple EMGs in the same sessions, we observed that single trial discrimination based on neuronal data continued to be highly significant even though

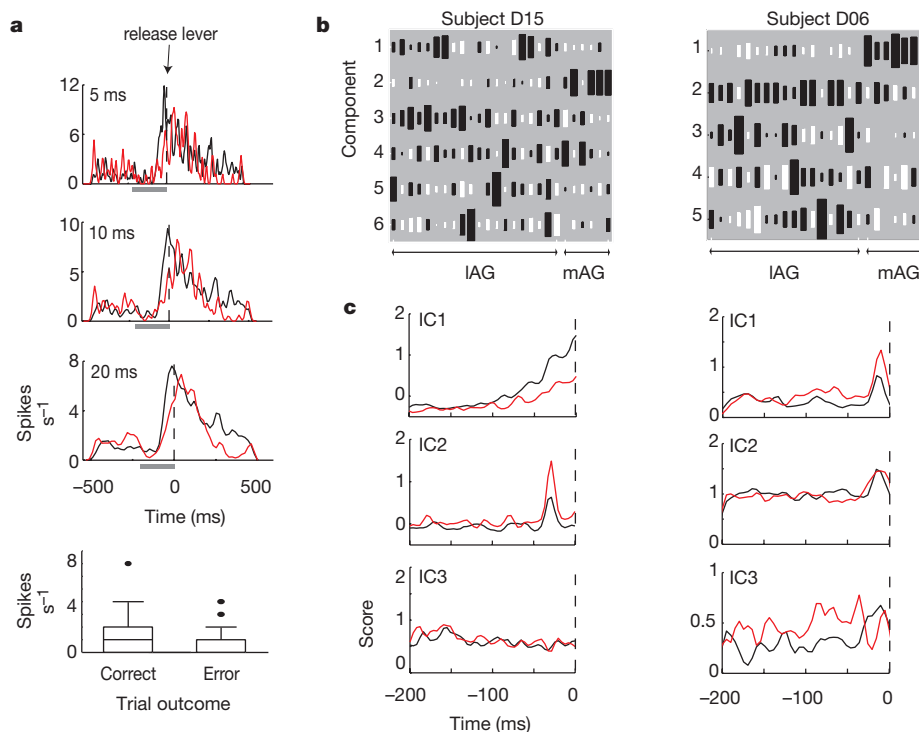


**Figure 3** Predictions of trial outcome were based on temporal patterns of firing and correlated activity. **a**, Temporal patterns of neuronal firing (about 5–10 ms) predicted correct (black) and error (red) trials better than average firing rates (box plots: box is interquartile range (IQR), line is median, and dots are extreme values, that is, greater than 1.5 times the IQR), which were not different on correct and error trials. **b,c**, Independent component analysis (ICA) detected correlations between subgroups of neurons (**b**) during

the final 200 ms before movement (data from two fully trained subjects). Neurons that fired together have the same colour boxes, and the size of the boxes reflects the correlation between the neurons. Trial outcomes were predicted significantly above chance due to the occurrence of different patterns of correlated firing (**c**) on correct (black) and error (red) trials.

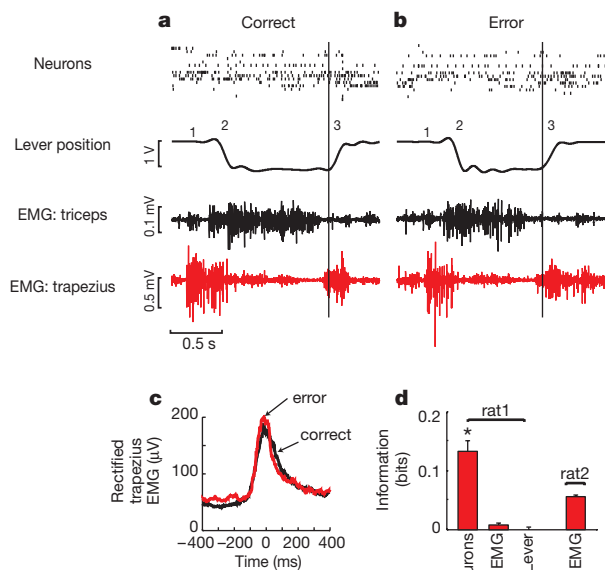


**Figure 4** Muscle activations and response kinematics were similar on correct and error trials. **a**, Correct trial. **b**, Error trial. The triceps brachii (black) showed increased EMG activity during lever pressing, while the trapezius (red) showed increased activity as the limb was placed on the lever and during lever release (vertical lines). Behavioural events: 1, placing paw on lever; 2, pressing lever; 3, releasing lever. **c**, Average EMG activations and lever kinematics were equivalent on correct (black) and error (red) trials. **d**, Neuronal ensemble activity recorded in one of these rats provided far more information (asterisk,  $P < 0.01$ ) than the multiple EMG or lever position signals, which did not predict trial outcome better than expected by chance ( $P > 0.1$ ).

EMGs never achieved significance (Fig. 4c). In summary, these control experiments indicate that the improvement in predictions of trial outcomes over the learning period were not because of differences in the movements between correct and error trials.

Our results demonstrate that the ability of neuronal ensembles in the motor cortex to encode sensorimotor contingencies increases during motor learning. We found that the average firing rate, temporal structure and correlated activity of neuronal ensembles in the motor cortex changes during learning to represent new behaviourally relevant information. As reproducible results were obtained in four rats by randomly sampling 20–30 neurons per animal, these changes probably involve widespread territories of the rat motor cortex. Based on these observations, we propose that new functional associations between subgroups of cortical neurons may emerge as animals learn the new sensorimotor contingencies that are required to solve motor tasks. □

**Methods**

For more detailed methods see Supplementary Information.

**Behavioural task**

We recorded neuronal responses during learning from four adult, male rats. Neuronal responses were recorded from two additional animals only after they were fully trained, and two more animals were used for control studies using EMG. The rats were moderately deprived of water and trained to press a lever and release it in response to a trigger stimulus for a liquid reward. The foreperiod was initially 250 ms and was incremented by 50–100 ms whenever the rats made three consecutive correct trials. Once the foreperiod was greater than 600 ms and the animal performed the task consistently, the foreperiod varied randomly between 400–800 ms. All events during training and recording were controlled by computer. Behaviour of all rats was monitored by a video system, and by a position sensor attached to the lever in the two rats used for EMG controls.

**Electrophysiological recordings**

All rats were treated in accordance with NIH guidelines. Procedures for chronically implanting arrays of microwires (NB Labs, Dennison, Texas) and data acquisition, using a Many Neuron Acquisition Program (Plexon, Dallas, Texas), are described elsewhere<sup>23</sup>.

After the completion of all experiments, select recording sites were marked with electrolytic lesions before formalin perfusion, and the locations of microwires were reconstructed using histological techniques.

Multiple bipolar patch electrodes (MicroProbe, Potomac, Maryland) were implanted subcutaneously into two rats to record EMG ensemble activity chronically<sup>24</sup>. In the first rat, we recorded the activity of the triceps brachii (action: elbow extension) and the thoracic portion of trapezius (rotation of the limb at the shoulder). In the second rat, we recorded EMG activity from the anterior portion of deltoideus and pectoralis in addition to trapezius and triceps. EMG signals were amplified (SA Instrumentation, Encinitas, California), filtered at 20–500 Hz and sampled at 1,000 Hz.

**Data analysis**

Our strategy for statistical analysis of neuronal ensemble data sets is described elsewhere<sup>18,25,26</sup>. Single trial classification based on average neuronal firing rates was assessed by first summing all spikes for each trial over a 200-ms interval before lever release. These spike counts were then fed into an artificial neural network (ANN) that used the learning vector quantization (LVQ) algorithm<sup>17</sup>. Training and testing of artificial neural networks were performed on each behavioural training session in each subject to obtain the numbers depicting single trial classification. Leave-one-out cross-validation<sup>27</sup> was used to estimate error rates and the confusion matrices for each data set. The degree to which confusion matrices from the ANNs differed significantly from chance was then evaluated using information theory<sup>19</sup> and permutation tests<sup>20</sup>, and was expressed as bits of information.

Peri-event histograms (1-ms bins) were constructed for the correct and error trials for the 200-ms interval before lever release. The spike trains were then smoothed over 5-, 10- or 20-ms intervals by low-pass filtering and re-sampling (Fig. 3a). Firing patterns associated with correct and error trials were identified for each neuron using a wavelet-based method<sup>28</sup>, which essentially identified temporally specific, salient features in the data and thereby reduced the number of variables used to train the ANNs. Classification using the wavelet features was done as described above.

Independent component analysis (ICA) was used to assess how well correlated activity among different groups of cortical neurons predicted single trial outcome<sup>22</sup>. First, principal component analysis<sup>29</sup> was used to reduce the dimensionality of data from 200-ms intervals before lever release. An extended independent component algorithm<sup>21</sup> was then used to rotate the weights for the largest principal components to make the functions as statistically independent as possible. Scores for the resulting independent components were then computed for each 1-ms interval. These scores were then preprocessed with the wavelet algorithm and analysed with the same artificial neural network methods as described above. To test the notion that the ICA procedure detected correlated firing, the spike trains were decorrelated using a spike-shifting procedure described elsewhere<sup>22</sup>. Single trial classification based on digitally rectified EMG activity or lever position data was done using the same procedures as for the neuronal spike trains.

Received 8 December 1999; accepted 3 April 2000.

- Mitz, A. R., Godschalk, M. & Wise, S. P. Learning-dependent neuronal activity in the premotor cortex: activity during the acquisition of conditional motor associations. *J. Neurosci.* **11**, 1855–1872 (1991).
- Germain, L. & Lamarre, Y. Neuronal activity in the motor and premotor cortices before and after learning the associations between auditory stimuli and motor responses. *Brain Res.* **611**, 175–179 (1993).
- Chen, L. L. & Wise, S. P. Neuronal activity in the supplementary eye field during acquisition of conditional oculomotor associations. *J. Neurophysiol.* **73**, 1101–1121 (1995).
- Chen, L. L. & Wise, S. P. Supplementary eye field contrasted with the frontal eye field during acquisition of conditional oculomotor associations. *J. Neurosci.* **73**, 1122–1134 (1995).
- Chen, L. L. & Wise, S. P. Evolution of directional preferences in the supplementary field acquisition of conditional oculomotor associations. *J. Neurosci.* **16**, 3067–3081 (1996).
- Chen, L. L. & Wise, S. P. Conditional oculomotor learning: population vectors in the supplementary eye field. *J. Neurophysiol.* **78**, 1166–1169 (1997).
- Georgopoulos, A. P. *et al.* Primate motor cortex and free arm movements to visual targets in three-dimensional space. II. coding of the direction of movement by a neuronal population. *J. Neurosci.* **8**, 2928–2938 (1988).
- Shadlen, M. N. & Newsome, W. T. Noise, neural code and cortical organization. *Curr. Opin. Neurobiol.* **4**, 569–579 (1994).
- Murthy, V. N. & Fetz, E. E. Coherent 25- to 35-Hz oscillations in the sensorimotor cortex of awake behaving monkeys. *Proc. Natl Acad. Sci. USA.* **89**, 5670–5674 (1992).
- Nicolelis, M. A. L. *et al.* Sensorimotor encoding by synchronous neural ensemble activity at multiple levels of the somatosensory system. *Science* **268**, 1353–1358 (1995).
- Donoghue, J. P. *et al.* Neural discharge and local field potential oscillations in primate motor cortex during voluntary movements. *J. Neurophysiol.* **79**, 159–173 (1998).
- Seidemann, E. *et al.* Simultaneously recorded single units in the frontal cortex go through sequences of discrete and stable states in monkeys performing a delayed localization task. *J. Neurosci.* **16**, 752–768 (1996).
- Riehle, A. *et al.* Spike synchronization and rate modulation differentially involved in motor cortical function. *Science* **278**, 1950–1953 (1997).
- Hatsopoulos, N. G. *et al.* Information about movement direction obtained from synchronous activity of motor cortical neurons. *Proc. Natl Acad. Sci. USA* **95**, 15706–15711 (1998).
- Maynard, E. M. *et al.* Neuronal interactions improve cortical population coding of movement direction. *J. Neurosci.* **19**, 8083–8093 (1999).
- Almaric, M. & Koob, G. F. Depletion of dopamine in the caudate nucleus but not in the nucleus accumbens impairs reaction time performance in rats. *J. Neurosci.* **7**, 2129–2134 (1987).
- Kohonen, T. *Self-organizing Maps* (Springer, New York, 1997).
- Nicolelis, M. A. L., Stambaugh, C. R., Brisben, A. & Laubach, M. in *Methods for Simultaneous Multisite Neural Ensemble Recordings in Behaving Primates* (ed. Nicolelis, M. A. L.) 121–156 (CRC, Boca Raton, 1999).

19. Krippendorff, K. *Information Theory: Structural Models for Qualitative Data* (Sage, Thousand Oaks, California, 1986)
20. Efron, B. & Tibshirani, R. *An Introduction to the Bootstrap*. (Chapman & Hall, New York, 1994).
21. Lee, T. W., Girolami, M. & Sejnowski, T. J. Independent component analysis using an extended infomax algorithm for mixed subgaussian and supergaussian sources. *Neural Comput.* **11**, 417–441 (1999).
22. Laubach, M., Shuler, M. & Nicolelis, M. A. L. Independent component analyses for quantifying neuronal ensemble interactions. *J. Neurosci. Meth.* **94**, 141–154 (1999).
23. Nicolelis, M. A. L. *et al.* Reconstructing the engram: simultaneous, multiple site, many single neuron recordings. *Neuron* **18**, 529–537 (1997).
24. Loeb, G. E. & Gans, C. *Electromyography for Experimentalists* (Univ. of Chicago Press, Chicago, 1986).
25. Nicolelis, M. A. L. *et al.* Simultaneous encoding of tactile information by three primate cortical areas. *Nature Neurosci.* **1**, 621–630 (1998).
26. Ghazanfar, A. A., Stambaugh, C. R. & Nicolelis, M. A. L. Multiple strategies for encoding tactile information by somatosensory thalamocortical ensembles. *J. Neurosci.* (in the press).
27. Mosteller, F. & Tukey, J. W. *Data Analysis and Regression: A Second Course in Statistics* (Addison-Wesley, Reading, Massachusetts, 1977).
28. Buckheit, J. & Donoho, D. Improved linear discrimination using time-frequency dictionaries. *Proc. SPIE* **2569**, 540–551 (1995).
29. Reyment, R. A. & Jöreskog, K. G. *Applied Factor Analysis in the Natural Sciences* (Cambridge Univ. Press, New York, 1993).

Supplementary information is available on Nature's World-Wide Web site (<http://www.nature.com>) or as paper copy from the London editorial office of Nature.

#### Acknowledgements

We thank P. Beck, D. Cohen, D. Katz, D. Krupa, M. Shuler and B. Storey-Laubach for comments on the manuscript. The work was supported by grants from the National Institute of Health (M.L. and M.A.L.N.), the National Science Foundation, the Defense Advanced Research Project Agency, the Office of Naval Research, and the Human Frontiers and Whitehall Foundations (M.A.L.N.). J.W. was supported by the Swedish Foundation for International Cooperation in Research and Higher Education and by the Swedish Medical Research Council.

Correspondence and requests for materials should be addressed to: M.L. (e-mail: [laubach@neuro.duke.edu](mailto:laubach@neuro.duke.edu)).

## An electroneutral sodium/bicarbonate cotransporter NBCn1 and associated sodium channel

Inyeong Choi\*, Christian Aalkjaer†, Emile L. Boulpaep\* & Walter F. Boron\*

\* Department of Cellular and Molecular Physiology, Yale University School of Medicine, New Haven, Connecticut 06520, USA

† Department of Physiology and Danish Biomembrane Research Centre, University of Aarhus, Aarhus, DK-8000, Denmark

Two electroneutral, Na<sup>+</sup>-driven HCO<sub>3</sub><sup>-</sup> transporters, the Na<sup>+</sup>-driven Cl<sup>-</sup>/HCO<sub>3</sub><sup>-</sup> exchanger and the electroneutral Na<sup>+</sup>/HCO<sub>3</sub><sup>-</sup> cotransporter, have crucial roles in regulating intracellular pH in a variety of cells, including cardiac myocytes<sup>1,2</sup>, vascular smooth-muscle<sup>3,4</sup>, neurons<sup>5</sup> and fibroblasts<sup>6</sup>; however, it is difficult to distinguish their Cl<sup>-</sup> dependence in mammalian cells. Here we report the cloning of three variants of an electroneutral Na<sup>+</sup>/HCO<sub>3</sub><sup>-</sup> cotransporter, NBCn1, from rat smooth muscle. They are 89–92% identical to a human skeletal muscle clone<sup>7</sup>, 55–57% identical to the electrogenic NBCs and 33–43% identical to the anion exchangers<sup>8</sup>. When expressed in *Xenopus* oocytes, NBCn1-B (which encodes 1,218 amino acids) is electroneutral, Na<sup>+</sup>-dependent and HCO<sub>3</sub><sup>-</sup>-dependent, but not Cl<sup>-</sup>-dependent. Oocytes injected with low levels of NBCn1-B complementary RNA exhibit a Na<sup>+</sup> conductance that 4,4-diisothiocyanatostilbene-2,2'-disulphonate stimulates slowly and irreversibly.

We designed degenerate primers to identify NBC-related complementary DNAs from rat aorta based on an amino-acid sequence

comparison of several NBCs<sup>9–12</sup>, a *Caenorhabditis elegans* expressed sequence tag (EST) clone (GenBank accession number Z75541) and rat anion exchangers<sup>13</sup>. We cloned a 294-base pair (bp) polymerase chain reaction (PCR) product, the deduced amino-acid sequence of which is 76% identical to electrogenic renal and pancreatic NBCs. We obtained the 5' end of the open reading frame by 5' rapid amplification of cDNA ends (RACE) of aorta RNA, and obtained the 3' end by performing PCR on a pulmonary-artery cDNA library.

To test whether our three cDNA fragments represent a single transcript, we performed PCR with reverse transcription (RT-PCR) using total RNA from rat aorta and primers designed to amplify the entire coding region. We obtained three distinct, full-length clones (NBCn1-B, C and D). Compared with the NBCn1-D (Fig. 1a), NBCn1-B lacks a 36-residue 'B' domain near the carboxy terminus, and NBCn1-C lacks a 14-residue 'A' domain near the amino terminus (Fig. 1b). The rat NBCn1s are 89–92% identical to a human skeletal-muscle cDNA ('NBC-3/Pushkin')<sup>7</sup>, which we propose to call NBCn1-A. Figure 1a compares the deduced amino-acid sequence of NBCn1-D with the electrogenic rat-kidney NBC (57% identity)<sup>10</sup> and rat AE2 (33–43% identity)<sup>13</sup>. Figure 1c shows the relationships among selected members of the HCO<sub>3</sub><sup>-</sup> transporter superfamily. The identity between the NBCn1s and electrogenic NBCs is a fairly uniform 62% along the membrane-spanning regions, but falls off sharply (< 20%) at the amino and carboxy termini. The hydropathy plot of NBCn1-D is similar to that of a typical electrogenic NBC (Fig. 1d).

A northern blot of rat tissues (Fig. 2a), using a probe corresponding to a region common to the NBCn1s, shows substantial hybridization to a 7.5-kilobase (kb) transcript in spleen and a 4.1-kb transcript in testis. The signals are moderate in several other tissues, but undetectable in skeletal muscle. Using primers based on conserved NBCn1 sequences, we obtained a PCR product of the predicted size from spleen, aorta and brain (Fig. 2b).

To test the functional properties, we injected NBCn1-B cRNA into oocytes, and used microelectrodes to monitor membrane potential ( $V_m$ ) and intracellular pH ( $pH_i$ ). Oocytes expressing NBCn1-B differ in two principal ways from controls. First, the resting  $V_m$  was  $-30 \pm 1$  mV ( $n = 32$ ),  $\sim 30$  mV more positive ( $P < 0.001$ ) than in control oocytes ( $-60 \pm 3$  mV,  $n = 9$ ). Second, the average initial  $pH_i$  was  $7.46 \pm 0.01$  ( $n = 29$ ), 0.12 units higher ( $P < 0.01$ ) than in controls ( $7.34 \pm 0.03$ ,  $n = 5$ ). Thus, NBCn1-B mediates net HCO<sub>3</sub><sup>-</sup> influx with the trace amounts of HCO<sub>3</sub><sup>-</sup> present in the incubation medium.

In control oocytes injected with water (Fig. 3a), applying 1.5% CO<sub>2</sub>/10 mM HCO<sub>3</sub><sup>-</sup> caused a rapid  $pH_i$  fall, followed by a long period of stability. In oocytes injected with NBCn1-B cRNA (Fig. 3b), adding CO<sub>2</sub>/HCO<sub>3</sub><sup>-</sup> to the bath caused the usual  $pH_i$  fall, followed by a rise owing to HCO<sub>3</sub><sup>-</sup> uptake. More importantly, CO<sub>2</sub>/HCO<sub>3</sub><sup>-</sup> did not affect  $V_m$ . In oocytes expressing an electrogenic NBC, CO<sub>2</sub>/HCO<sub>3</sub><sup>-</sup> elicits a rapid hyperpolarization, which may be as large as 80 mV (refs 9,10,12). Thus, NBCn1-B mediates electroneutral Na<sup>+</sup>/HCO<sub>3</sub><sup>-</sup> cotransport (that is, Na<sup>+</sup>:HCO<sub>3</sub><sup>-</sup> stoichiometry of 1:1). Removing Na<sup>+</sup> from the bath converted the  $pH_i$  recovery to an acidification (Fig. 3b), consistent with reversal of electroneutral Na<sup>+</sup>/HCO<sub>3</sub><sup>-</sup> cotransport. Note that Na<sup>+</sup> removal hyperpolarized oocytes expressing NBCn1-B by  $25 \pm 1$  mV ( $n = 10$ ), much larger than the  $11 \pm 1$  mV ( $n = 9$ ) in controls ( $P < 0.001$ ).

When we acidified oocytes expressing NBCn1-B with butyric acid rather than CO<sub>2</sub> (Fig. 3c),  $pH_i$  failed to recover in the presence of Na<sup>+</sup>, and failed to acidify in the absence of Na<sup>+</sup>. Thus, transport by NBCn1-B requires HCO<sub>3</sub><sup>-</sup> in both the inward and outward directions. Note also that Na<sup>+</sup> removal in butyrate caused the same large hyperpolarization as in CO<sub>2</sub>/HCO<sub>3</sub><sup>-</sup>.

To test whether NBCn1-B encodes a Na<sup>+</sup>-driven Cl<sup>-</sup>/HCO<sub>3</sub><sup>-</sup> exchanger, we removed bath Cl<sup>-</sup> in the presence of CO<sub>2</sub>/HCO<sub>3</sub><sup>-</sup> (data not shown); however, Cl<sup>-</sup> removal did not speed the  $pH_i$